Cyclo[18]Carbon: Insight into Electronic Structure, Aromaticity and Surface Coupling

Gleb V. Baryshnikov,[a,b,*] Rashid R. Valiev,[c,d] Artem Kuklin,[a,e] Dage Sundholm,[d] and Hans Ågren[a,f]

[a] *Division of Theoretical Chemistry and Biology, School of Engineering Sciences in Chemistry, Biotechnology and Health, KTH Royal Institute of Technology, 10691, Stockholm, Sweden*

[b] *Department of Chemistry and Nanomaterials Science, Bohdan Khmelnytsky National University, 18031, Cherkasy, Ukraine*

[c] *Research School of Chemistry & Applied Biomedical Sciences, National Research Tomsk Polytechnic University, Lenin Avenue 30, Tomsk 634050, Russia*

[d] *Department of Chemistry, Faculty of Science, University of Helsinki, FIN-00014, Helsinki, Finland*

[e] *Siberian Federal University, 79 Svobodniy pr., Krasnoyarsk 660041, Russia*

[f] *College of Chemistry and Chemical Engineering, Henan University, Kaifeng, Henan 475004, P.R. China*

ABSTRACT: Cyclo[18]carbon (C_{18}) is studied computationally at density functional theory (DFT) and *ab initio* levels to obtain insights into its electronic structure, aromaticity, and adsorption properties on the NaCl surface. DFT functionals with a small amount of Hartree-Fock exchange as well as CASPT2 calculations fail to determine the experimentally observed polyyne molecular structure revealing a cumulene-type geometry. Exchange-correlation functionals with a large amount of Hartree-Fock exchange as well as *ab initio* CASSCF calculations yield the polyyne structure is a ground state while the cumulene structure corresponds to the transition state between the two inverted polyyne structures through the Kekule distortion. The polyyne and the cumulene structures are found to be doubly Hückel aromatic. The calculated adsorption energy of cyclo[18]carbon on the NaCl surface is small (37 meV/C) and almost the same for both structures implying that the surface does not stabilize a particular geometry.

Carbon is one of the most diverse elements of the periodic table with respect to the possible allotropes.[1,2] Among them sp^3-hybridized diamond, multilayered sp^2-hybridized graphite and monolayer graphene, fullerenes and nanotubes, sp-hybridized carbine, and linear polyynes are still the most attractive materials as unique objects for practical applications and theoretical surveys.[3–5] The number of hypothetically predicted carbon allotropes reaches more than five hundred different structures in accordance with the SACADA database[6] last updated on May 2017. Nevertheless, carbon allotropes are still in focus of synthetic attempts and theoretical predictions.[7–13] One of the most impressive recent achievements in this field is the successful synthesis and characterization of the closed-circle polyyne containing 18 sp-hybridized carbon atoms and called cyclo[18]carbon.[14] About 50 years ago, Hoffmann[15] predicted the special "double" aromaticity of the cyclo[18]carbon ring through the delocalization of two scaffolds of 18 π-electrons oriented in the plane of C_{18} ring ($18\pi_{in}$) and perpendicular to it ($18\pi_{out}$, Figure 1).

Here, we support the notion of Torelli and Mitas by demonstrating that increasing the Hartree-Fock exchange part in an exchange-correlation functional leads to the experimentally observed polyyne structure of cyclo[18]carbon. The use of multiconfiguration perturbation theory at the XMC-QDPT2 level of theory for considering correlation effects also results in the incorrect global minimum of cumulenic structure for cyclo[18]carbon, which agrees with Houk-Planner conclusions. In contrast, *ab initio* CASSCF calculations exhibit the correct structure suggesting limitations in the applicability of the multiconfiguration PT2 correlation scheme on cyclo[18]carbon. We are also utilized the gauge-including magnetically induced currents (GIMIC) approach[30,31] to investigate the magnetically induced current density and the "double" aromaticity of cyclo[18]carbon beyond the previously published NICS[23] and ipsocentric CTOCD-DZ[24] (continuous transformation of origin of current density – diamagnetic zero) studies. Finally, the idea that the cumulenic structure of cyclo[18]carbon is the ground-state structure in the gas phase in isolated form, while surface interaction may induce stabilization of the polyyne-type structure has been investigated and disproved by simulations of cyclo[18]carbon adsorption on the NaCl (100) surface within periodic boundary conditions (PBC)

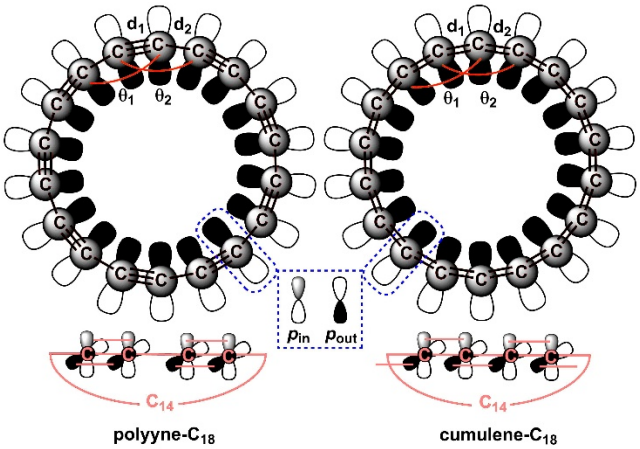

Figure 1. Polyyne and cumulene structure of cyclo[18]carbon molecule.

.

Table 1. Selected structural parameters of the ground state polyyne and transition state cumulene forms of cyclo[18]carbon calculated at the different levels of theory.

	polyyne (C_{9h}, ground state)					cumulene (C_{9h}, transition state)				
	d_1, Å	d_2, Å	θ_1,°	θ_2,°	ω_1, cm^{-1}	d_1, Å	d_2, Å	θ_1,°	θ_2,°	ω_1 cm^{-1}
M06-2X	1.226	1.346	160	160	59	1.278	1.277	163	157	1683i
BMK	1.235	1.332	160	160	61	1.279	1.278	163	157	1200i
BHandHLYP	1.223	1.346	159	161	59	1.271	1.271	169	151	1553i
wB97XD	1.223	1.346	159	161	59	1.277	1.277	169	151	1743i
CASSCF(8,8)	1.199	1.356	160	160	59	1.265	1.265	163	159	1900i

The following exchange-correlation functionals (see supporting information (SI) for details) with increased percentage of Hartree-Fock exchange (HFE) relative to the common B3LYP functional (20% HFE) have been selected to probe the ground state structure of cyclo[18]carbon: BMK (42% HF), M06-2X (54% HFE), BHandHLYP (50% HFE) and wB97XD (22% short-range HFE, range separation parameter γ=0.2). All of them provide the polyyne-type ground state structure of cyclo[18]carbon of the C_{9h} symmetry point group with alternating single and triple C-C bonds (the corresponding structural parameters are collected in Table 1). No significant bond angles alternating θ_1 and θ_2 was observed. The typical deviations are less than 1°. All calculated vibrational frequencies were found to be real (ω_1 is real and positive in Table 1) for all cases of polyyne cyclo[18]carbon indicating the true energy minimum whereas one imaginary frequency was obtained for the cumulene structure.

In favor of the hypothesis that increased contribution of HFE affects the ground-state geometry of large cyclo[4N+2]carbon molecules (N=4-8), we refer to the study by Remya and Suresh[23]. They used the meta-GGA M06L local functional with zero 0% HFE, which revealed a cumulenic ground-state structure for the studied cyclo[4N+2]carbons (N=4-8) including cyclo[18]carbon. In order to estimate the threshold HFE value sufficient to obtain the correct bond alternation in cyclo[18]carbon in the hybrid functional, we performed structural relaxations using two DFT levels (B3LYP/6-311++G(d,p) and HSE06 with plane wave (PW) basis set as described in details in SI) varying the HFE part from 0 to 100%. We found that 37% HFE contribution at the B3LYP/6-311++G(d,p) and 32% HFE within HSE06/PW levels are enough to reproduce the experimentally observed polyyne bond-length alternation of cyclo[18]carbon. Other hybrid functionals used in this work reproduce the HFE trend obtained with the B3LYP and HSE06 reference functionals (Figure S1).

The attempts to optimize the cumulenic-type geometry of cyclo[18]carbon within BMK, M06-2X, BHandHLYP, wB97XD functionals and CASSCF(8,8) calculations with different symmetry constraints always yielded a saddle point with the one or few imaginary frequencies. The calculations suggest that the cumulene-type geometry might be a transition state structure for a bond shift between two polyyne forms of cyclo[18]carbon with inverted ordering of single and triple bonds (both of C_{9h} symmetry, Figure 2). Indeed, QST3 optimization of the transition state structure for such a bond shift resulted in a bond-angle alternating cumulene-type geometry (Table 1) of the same C_{9h} symmetry with one imaginary frequency corresponding to the Kekule-type in-plane C-C stretching vibrations (Figure 2). The calculated energy barrier for the inversion process depends on the method. The BMK functional underestimates the bond shift barrier in comparison to the other levels of theory, demonstrating a barrier of only +3.5 kcal mol^{-1}, while the rest of the functionals (M06-2X, BHandHLYP, wB97XD) as well as CASSCF(8,8) calculations, yield very similar barrier heights of 8.8-12.1 kcal/mol (Figure 2). The CASSCF calculations show that the predominant weight of a closed-shell singlet determinant for the polyyne and cumulenic structures is 0.95, implying that single-reference approaches should be applicable. Employing the XMC-QDPT2 approach to find the equilibrium cyclo[18]carbon structure resulted in the same structure with equal C-C bond lengths independently on which structural type (polyyne or cumulenic) was the initial geometry. Varying the basis set within the XMC-QDPT2 scheme did not affect the results.

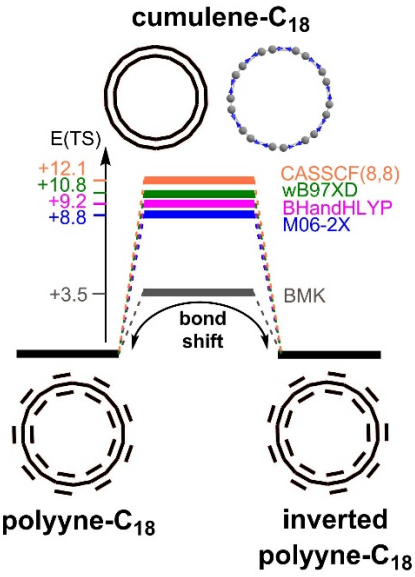

Figure 2. Bond shift mechanism in polyyne cyclo[18]carbon through the cumulene transition state mediated by Kekule vibration. The barriers are given in kcal mol^{-1}.

Using the M062X/6-311++G(d,p) optimized ground-state polyyne structure and the transition-state cumulene geometry, we performed calculations of the magnetically induced ring current strength using the GIMIC approach (see details in the SI). We found that applying an external magnetic field perpendicular to the molecular plane of cyclo[18]carbon induces a strong diatropic ring current of 29 nA T^{-1} showing that polyyne cyclo[18]carbon is aromatic in agreement with NICS and ipsocentric CTOCD-DZ calculations[23,24] and the Hückel (4N+2) rule[15]. For comparison, benzene sustains a net diatropic ring current about 12 nA T^{-1}.[31] The signed modulus of the magnetically induced current density (Figure 3) shows that diatropic ring current in polyyne-type cyclo[18]carbon originates from the two scaffolds of 18 π-electrons oriented in- and out- of molecular plane proving the double aromaticity idea proposed by Hoffman more than 50 years ago.[15] Calculating the ring current strength within reduced contours that cover particular in- and out-of-plane delocalization areas (see details in SI) shows the efficient delocalization of the 18π_{out} electrons (I_{out} = 21.8 nA T^{-1}) and less the efficient delocalization of 18π_{in} electrons (I_{in} = 7.2 nA

T^{-1}) due to the perpendicular alignment of these orbitals.[24] The cumulene-type TS structure sustains much higher net diatropic current (73.2 nA T^{-1}) due to the more efficient overlap and delocalization of the π_{in} and π_{out} orbitals. The strengths of the I_{in} and I_{out} currents for the cumulene structure were found to be the same (both equal to 36.6 nA T^{-1}) meaning that the π_{in} and π_{out} orbitals are identical with respect to the orbital delocalization.

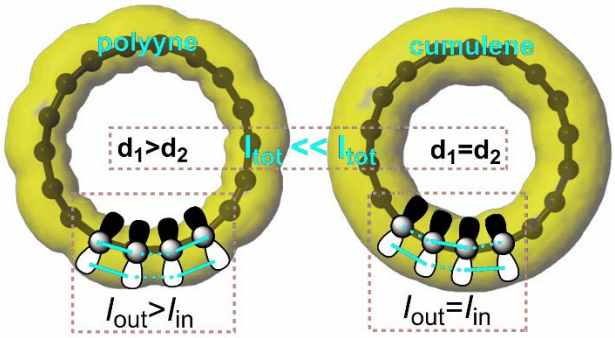

Figure 3. The signed modulus of the magnetically induced current densities for the polyyne and cumulene cyclo[18]carbon.

In order to elucidate the hypothesis that the cumulene type geometry is a gas phase global minimum structure, while the polyyne geometry can only exist on the NaCl surface due to extra stabilization effects (relative to cumulenic one), we performed calculations of the adsorption of polyyne- and cumulene-type cyclo[18]carbon on a NaCl (100) surface using the PBC approximation (see SI for details). The initial 4 × 4 thin-film models of $Na_{54}Cl_{54}$ superstructure consisting of three atomic layers were obtained from a well-converged NaCl unit cell and then relaxed. We found that the unit cell is large enough to simulate cyclo[18]carbon adsorption on the NaCl surface avoiding spurious interactions between the molecules with an effective separation distance of 9.58 Å between nearest neighboring cyclo[18]carbon molecules. The simulated superstructure is shown in Figure 4a. Regardless of the assumed initial cyclo[18]carbon geometry (cumulenic or polyynic), the final optimized geometry was found to be of cumulene type when the PBE functional with 0% of HFE was utilized. This confirms once again that functionals like PBE without enough contribution of HFE cannot properly describe geometry and electronic structure of cyclo[18]carbon.

To estimate the adsorption parameters of polyyne cyclo[18]carbon, we used its equilibrium structure obtained at the CASSCF(8,8) level and then fixed all carbon positions but allowed to completely relax the NaCl (100) substrate. Similarly we calculated the cumulene type but allowing to relax all atoms. We found, that the formation of the C_{18}/NaCl heterostructure does not play any significant role in the stabilization of the polyynic structure. The adsorption energies were found to be almost equivalent (37 meV/C) for both cumulenic and polyynic structures. It confirms that there is no surface-induced transition between polyyne and cumulene structures, because the adsorption energies of both structures are the same. Accounting for the very weak interaction between cyclo[18]carbon and NaCl it is evident that the molecules can freely move along the NaCl surface even at very low temperatures, which is in agreement with experimental observations.[14] Indeed, calculations using the nudge elastic band (NEB) method[32] yield a very small energy barrier of 30 meV for the cyclo[18]carbon mobility on the NaCl surface (Figure 4b).

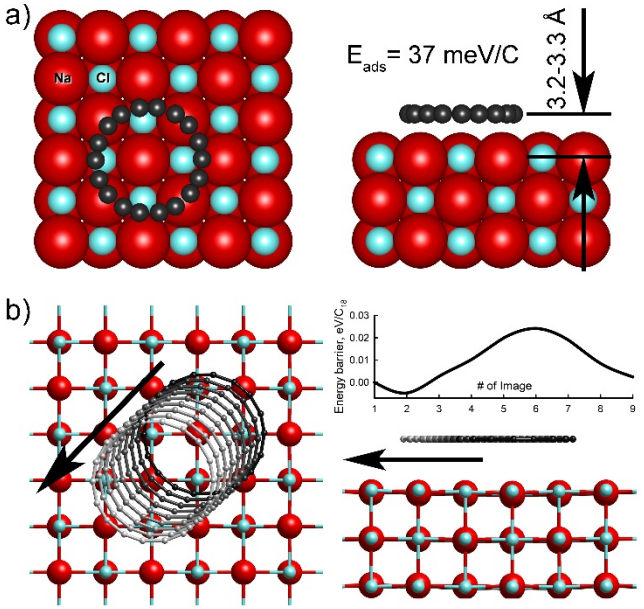

Figure 4. (a) Top (left) and side (right) views of the NaCl supercell with adsorbed cyclo[18]carbon. (b) Results of the NEB simulation of the cyclo[18]carbon mobility along the NaCl surface. The arrows depict the direction of cyclo[18]carbon molecule movement during NEB cycle.

In conclusion, the recently synthesized cyclo[18]carbon molecule has been studied computationally at the DFT and CASSCF levels of theory in order to finally confirm that the polyyne structure is the global minimum. The cumulene-type structure of cyclo[18]carbon is found to be a transition state for the single-triple bond inversion process. This interconversion is mediated by the Kekule-type stretching vibration with the estimated energy barrier of around 10 kcal mol^{-1}. An extended amount of Hartree–Fock exchange in the employed functional is crucial for obtaining the experimentally observed polyyne structure of cyclo[18]carbon. The double aromaticity of both polyyne and cumulenic cyclo[18]carbon has been investigated by gauge-including magnetically induced currents calculations, which predict that the bond-alternating alternating polyyne structure is less aromatic than non-alternating transition-state structure due to a less efficient overlap of π_{in} and π_{out} orbitals of the polyyne structure. Two molecular structures of cyclo[18]carbon have identical adsorption energies on the NaCl surface, suggesting that there is no extra stabilization favoring polyyne structure as compared to the cumulenic one. NEB simulations show that cyclo[18]carbon can move almost without any barrier on the NaCl (100) surface, which is in agreement with experimental data.

ASSOCIATED CONTENT

Supporting Information

The Supporting Information is available free of charge on the ACS Publications website at DOI: 10.1021/jacs.XXXXXXX. Computational details and corresponding references on the employed methods, bond length dependence on the percentage of HFE contribution within the HSE06 and B3LYP hybrid functionals (PDF).

AUTHOR INFORMATION

Corresponding Author

E-mail: glibar@kth.se

Notes

The authors declare no competing financial interests.

ACKNOWLEDGMENT

This work was supported by the Olle Engkvist Byggmästare foundation (contract no. 189-0223) and by the Ministry of Education and Science of Ukraine (project no. 0117U003908). The calculations were performed with computational resources provided by the High-Performance Computing Center North (HPC2N) in Umeå, Sweden, through the project ''Multiphysics Modeling of Molecular Materials'' SNIC 2018-2-38. The GIMIC calculations were carried out using SKIF supercomputer at the Tomsk State University. A.V.K. acknowledges the support of the Russian Science Foundation (Project No. 19-73-10015). R.R.V. thanks the Academy of Finland (1325369) and is also thankful to the Tomsk Polytechnic University Competitiveness Enhancement Program (VIU-RSCABS-142/2019).

REFERENCES

(1) Hirsch, A. The Era of Carbon Allotropes. *Nat. Mater.* **2010**, *9* (11), 868–871.

(2) Georgakilas, V.; Perman, J. A.; Tucek, J.; Zboril, R. Broad Family of Carbon Nanoallotropes: Classification, Chemistry, and Applications of Fullerenes, Carbon Dots, Nanotubes, Graphene, Nanodiamonds, and Combined Superstructures. *Chem. Rev.* **2015**, *115* (11), 4744–4822.

(3) Dunlap, R. A. Other Crystalline Allotropes of Carbon. In *Novel Microstructures for Solids*; IOP Publishing, 2018, 8-1–8-9

(4) Nasir, S.; Hussein, M. Z.; Zainal, Z.; Yusof, N. A. Carbon-Based Nanomaterials/Allotropes: A Glimpse of Their Synthesis, Properties and Some Applications. *Materials (Basel).* **2018**, *11* (2), 1–24.

(5) Pierson, H. O. *Handbook of Carbon, Graphite, Diamond, and Fullerenes : Properties, Processing, and Applications*; Noyes Publications, 1993.

(6) Hoffmann, R.; Kabanov, A. A.; Golov, A. A.; Proserpio, D. M. *Homo Citans* and Carbon Allotropes: For an Ethics of Citation. *Angew. Chemie Int. Ed.* **2016**, *55* (37), 10962–10976.

(7) Shu, C.-H.; Liu, M.-X.; Zha, Z.-Q.; Pan, J.-L.; Zhang, S.-Z.; Xie, Y.-L.; Chen, J.-L.; Yuan, D.-W.; Qiu, X.-H.; Liu, P.-N. On-Surface Synthesis of Poly(p-Phenylene Ethynylene) Molecular Wires via in Situ Formation of Carbon-Carbon Triple Bond. *Nat. Commun.* **2018**, *9* (1), 2322.

(8) Zuo, Z.; Wang, D.; Zhang, J.; Lu, F.; Li, Y. Synthesis and Applications of Graphdiyne-Based Metal-Free Catalysts. *Adv. Mater.* **2019**, *31* (13), 1803762.

(9) Kilde, M. D.; Murray, A. H.; Andersen, C. L.; Storm, F. E.; Schmidt, K.; Kadziola, A.; Mikkelsen, K. V.; Hampel, F.; Hammerich, O.; Tykwinski, R. R.; et al. Synthesis of Radiaannulene Oligomers to Model the Elusive Carbon Allotrope 6,6,12-Graphyne. *Nat. Commun.* **2019**, *10* (1), 3714.

(10) Wei, T.; Hauke, F.; Andreas, H. Covalent Inter-Synthetic-Carbon-Allotrope Hybrids. *Acc. Chem. Res.* **2019**, *52* (8), 2037–2045.

(11) Hu, J.; Wu, W.; Zhong, C.; Liu, N.; Ouyang, C.; Yang, H. Y.; Yang, S. A. Three-Dimensional Honeycomb Carbon: Junction Line Distortion and Novel Emergent Fermions. *Carbon* **2019**, *141*, 417–426.

(12) Cranford, S. W. When Is 6 Less than 5? Penta- to Hexa-Graphene Transition. *Carbon* **2016**, *96*, 421–428.

(13) Sundholm, D. C72: Gaudiene, a Hollow and Aromatic All-Carbon Molecule. *Phys. Chem. Chem. Phys.* **2013**, *15* (23), 9025.

(14) Kaiser, K.; Scriven, L. M.; Schulz, F.; Gawel, P.; Gross, L.; Anderson, H. L. An Sp-Hybridized Molecular Carbon Allotrope, Cyclo[18]Carbon. *Science.* **2019**, *1914* (August), eaay1914.

(15) Hoffmann, R. Extended Hückel Theory—v : Cumulenes, Polyenes, Polyacetylenes and Cn. *Tetrahedron* **1966**, *22* (2), 521–538.

(16) Diederich, F.; Rubin, Y.; Knobler, C. B.; Whetten, R. L.; Schriver, K. E.; Houk, K. N.; Li, Y. All-Carbon Molecules: Evidence for the Generation of Cyclo[18]Carbon from a Stable Organic Precursor. *Science* **1989**, *245* (4922), 1088–1090.

(17) Plattner, D. A.; Houk, K. N. C_{18} Is a Polyyne. *J. Am. Chem. Soc.* **1995**, *117* (15), 4405–4406.

(18) Torelli, T.; Mitas, L. Electron Correlation in C_{4N+2} Carbon Rings: Aromatic versus Dimerized Structures. *Phys. Rev. Lett.* **2000**, *85* (8), 1702–1705.

(19) Parasuk, V.; Almlof, J.; Feyereisen, M. W. The [18] All-Carbon Molecule: Cumulene or Polyacetylene? *J. Am. Chem. Soc.* **1991**, *113* (3), 1049–1050.

(20) Hutter, J.; Luethi, H. P.; Diederich, F. Structures and Vibrational Frequencies of the Carbon Molecules C_2-C_{18} Calculated by Density Functional Theory. *J. Am. Chem. Soc.* **1994**, *116* (2), 750–756.

(21) Ott, A. K.; Rechtsteiner, G. A.; Felix, C.; Hampe, O.; Jarrold, M. F.; Van Duyne, R. P.; Raghavachari, K. Raman Spectra and Calculated Vibrational Frequencies of Size-Selected C_{16}, C_{18}, and C_{20} Clusters. *J. Chem. Phys.* **1998**, *109* (22), 9652–9655.

(22) Boguslavskiy, A. E.; Ding, H.; Maier, J. P. Gas-Phase Electronic Spectra of C_{18} and C_{22} Rings. *J. Chem. Phys.* **2005**, *123* (3), 034305.

(23) Remya, K.; Suresh, C. H. Carbon Rings: A DFT Study on Geometry, Aromaticity, Intermolecular Carbon–Carbon Interactions and Stability. *RSC Adv.* **2016**, *6* (50), 44261–44271.

(24) Fowler, P. W.; Mizoguchi, N.; Bean, D. E.; Havenith, R. W. A. Double Aromaticity and Ring Currents in All-Carbon Rings. *Chem. - A Eur. J.* **2009**, *15* (28), 6964–6972.

(25) Arulmozhiraja, S.; Ohno, T. CCSD Calculations on C14, C18, and C22 Carbon Clusters. *J. Chem. Phys.* **2008**, *128* (11), 114301.

(26) Murphy, V. L.; Farfan, C.; Kahr, B. Chiroptical Structure-Property Relations in Cyclo[18]Carbon and Its in Silico Hydrogenation Products. *Chirality* **2018**, *30* (4), 325–331.

(27) Neiss, C.; Trushin, E.; Görling, A. The Nature of One-Dimensional Carbon: Polyynic versus Cumulenic. *ChemPhysChem* **2014**, *15* (12), 2497–2502.

(28) Saito, M.; Okamoto, Y. Second-Order Jahn-Teller Effect on Carbon 4N+2 Member Ring Clusters. *Phys. Rev. B* **1999**, *60* (12), 8939–8942.

(29) M.L. Martin, J.; El-Yazal, J.; François, J.-P. Structure and Vibrational Spectra of Carbon Clusters C_n (n=2–10, 12, 14, 16, 18) Using Density Functional Theory Including Exact Exchange Contributions. *Chem. Phys. Lett.* **1995**, *242* (6), 570–579.

(30) Jusélius, J.; Sundholm, D.; Gauss, J. Calculation of Current Densities Using Gauge-Including Atomic Orbitals. *J. Chem. Phys.* **2004**, *121* (9), 3952–3963.

(31) Fliegl, H.; Taubert, S.; Lehtonen, O.; Sundholm, D. The Gauge Including Magnetically Induced Current Method. *Phys. Chem. Chem. Phys.* **2011**, *13* (46), 20500.

(32) Henkelman, G.; Uberuaga, B. P.; Jónsson, H. A Climbing Image Nudged Elastic Band Method for Finding Saddle Points and Minimum Energy Paths. *J. Chem. Phys.* **2000**, *113* (22), 9901.

.

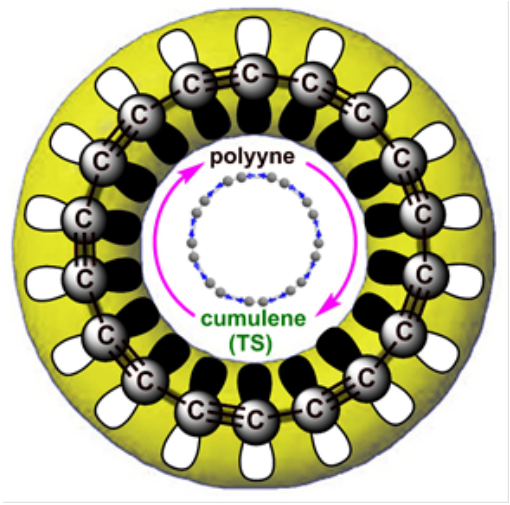

For Table of Contents Only